ACS APPLIED MATERIALS & INTERFACES

LETTER

www.acsami.org

Micelle-Mediated Synthesis of Single-Crystalline β(3C)-SiC Fibers via Emulsion Electrospinning

Seung-Hoon Choi,[†,‡] Doo-Young Youn,[†] Seong Mu Jo,[§] Seong-Geun Oh,[‡] and Il-Doo Kim*[,⊥]

[†]Optoelectronic Materials Center and [§]Polymer Hybrid Center, Korea Institute of Science and Technology, P.O. Box 131, Cheongryang, Seoul 130-650, Republic of Korea

[‡]Department of Chemical Engineering, Hanyang University, Seoul 133-791, Republic of Korea

[⊥]Department of Materials Science and Engineering, Korea Advanced Institute of Science and Technology, Daejeon 305-701, Republic of Korea

Supporting Information

ABSTRACT: Submicroscale SiC fiber mats were prepared by the electrospinning of an oil-in-water(O/W) precursor emulsion, a subsequent thermal curing treatment, and calcination at 1600 °C. Low-molecular-weight PCS micelles entrapped within an aqueous PVP matrix played an important role in forming the continuous and dense core structure, resulting in pure SiC fibers. The manipulation of SiC fiber diameters could be obtained via control of the micellar PCS concentration (10−30 wt %), enabling the production of dense and highly crystallized SiC fiber architectures with diameters ranging from 200 to 350 nm.

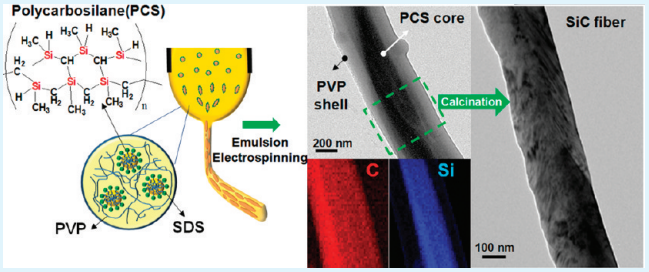

KEYWORDS: emulsion electrospinning, fiber, silicon carbide, core−sheath structure

Silicon carbide (SiC) is a chemically inert ceramic material that is widely used in applications requiring high mechanical endurance, high thermal conductivity, and high thermal stability. A wide range of synthetic routes for producing highly porous SiC nanostructures have been developed.[1] In particular, one-dimensional (1D) SiC building blocks have been explored extensively due to its potential applications in a diesel particulate filter (DPF)[2] and in high-power and high-frequency electronic devices.[3] The widespread interest in the 1D SiC architecture arises from its intriguing electrical and catalytic properties, which are closely related to its high surface-to-volume ratio and unusual transport properties connected to the quantum confinement effect or transport in fractal dimensions. Various approaches have been conducted to fabricated 1D SiC nanostructures such as nanowires, nanofiber and nanotubes. The methods include vapor−liquid−solid (VLS),[4] carbothermal reduction,[5] and template synthesis.[6] More recently, micrometer-scale SiC fibers were successfully prepared by the electrospinning, which is a very well reputed process for the simple and cost-effective preparation of various materials with 1D structure.[7,8] In most cases, the SiC fibers were synthesized by the electrospinning of a polycarbosilane (PCS, SiC precursor) solution dissolved in an aprotic solvent, e-beam irradiation and/or thermal curing, and a high-temperature annealing. The resultant SiC fibers exhibited a wide range of diameters (1−18 μm) and an inhomogeneous structure due to the relatively low molecular weight of conventional PCS (~3500 g/mol) precursor.[8] Although nanoscale (<100 nm) SiC fibers were also synthesized by carbothermally reducing polymer/Si precursor composite fibers obtained by electrospinning, the purity and uniformity issues of SiC fibers still remain significant challenges.[9]

In addition, emulsion electrospinning, which is based on the phase-separation of two different materials using a single nozzle, was introduced to fabricate core−sheath nanofibers.[10] Such core−sheath type of nanofibers reported thus far were mainly based on the encapsulation of hydrophilic drug reservoirs within thin hydrophobic polymer fibers using W/O (water-in-oil) emulsion concept whose target applications are mostly drug delivery or tissue engineering.[10e,f] However, to the best of our knowledge, there are no reports in the literature on the fabrication of ultrathin SiC fibers with high purity via emulsion electrospinning although earlier works have reported on potential feasibility for the synthesis of porous CeO_x/SiC[11] and SiO_2/SiC[12] nanocomposites using microemulsion precursors. In this work, we report single-crystalline SiC submicrofibers fabricated via electrospinning of an oil in water microemulsion including hydrophobic micelle droplets (PCS solution) entrapped within an aqueous poly (vinylpyrrolidone) (PVP) solution. Here, inner droplet (core) is a PCS fluid dissolved in toluene and the outer sheath is a PVP solution dissolved in water. Following high-temperature calcination of the as-spun PCS/PVP composite fibers was conducted to eliminate the PVP matrix and crystallize

Received: February 9, 2011
Accepted: April 8, 2011
Published: April 08, 2011

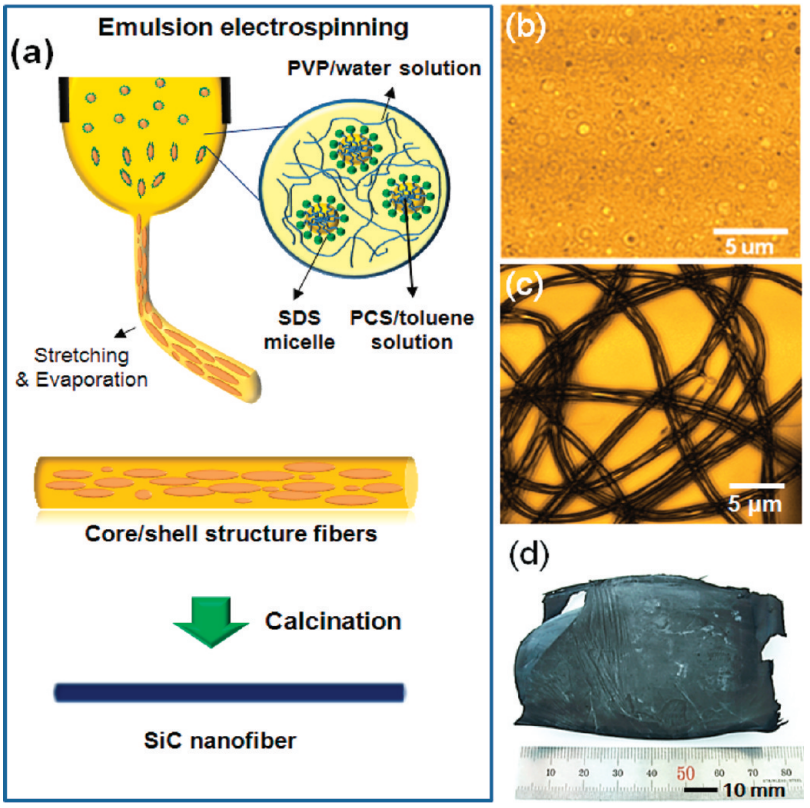

Figure 1. (a) Schematic processing procedure of SiC fibers through emulsion electrospinning using a single circular nozzle; (b) confocal microscopic image of PCS droplets(10 wt %) entrapped with in an aqueous PVP solution after 15 days; (c) confocal microscopic image of as-spun PCS/PVP composite fibers; (d) image of calcined SiC fiber mats.

the inner PCS core, resulting in β(3C)-SiC fiber mats (see the Supporting Information, Experimental Section). The manipulation of SiC fiber diameters could be obtained via control of the micellar PCS concentration, enabling the production of dense and highly crystallized fiber architectures.

The scheme in Figure 1a illustrates the overall procedure and the formation mechanism of the SiC fibers via the electrospinning of the O/W microemulsion. The obtained O/W emulsion was observed by a confocal microscope (Figure 1b). The diameters of the PCS micelles ranged from 210 to 1100 nm. The PCS droplet sizes did not change, even after 15 days, confirming the long-term stability of the PCS micelles. During the electrospinning of microemulsion solution, some PCS droplets were slightly stretched along with the elongation of outer PVP matrix[10a−d] and some PCS droplets were remained maintaining their original round shape as illustrated in Figure 1a. The size and stretched length of PCS droplets entrapped in as-spun PVP matrix can be manipulated by controlling the concentration of the emulsion droplets and the evaporation rate of the solvent. To obtain uniform and dense SiC fibers after solvent evaporation and high temperature calcination, the PCS polymer chains should have a certain degree of mobility to form continuous fibrous morphology in PVP matrix through interdiffusion of PCS segments.

In an effort to maximize the mobility of the PCS molecules, low-molecular-weight (800 g/mol) PCS was used, in this work, due to its straightforward migration and enhanced diffusion rate.[13] In contrast, the PVP fiber matrix should have high thermal stability while retaining its fiber shape until the PCS molecules completely diffuse and coalesce into the fibrous structure. For this reason, we introduced a thermal curing step at 200 °C in air to cross-link the PVP matrix. During thermal curing of PVP, partial surface oxidation of PCS was also occurred at the same time. Following a heat treatment above the thermal decomposition temperature (T_d, >220 °C in Ar or N_2) of PCS and PVP (see Figure S1 in the Supporting Information), a PCS fibril-core encapsulated by an outer PVP was obtained from the aggregation of PCS droplets in the PVP matrix. A further heat-treatment was then conducted to eliminate the PVP matrix and crystallize the PCS. Finally, freestanding nonwoven SiC fiber mats were successfully obtained (Figure 1d). To investigate the detailed information pertaining to the interior structure of PCS/PVP composite fibers with different PCS droplet concentration, TEM, FIB(focused ion beam)-SEM and EDS analyses were carried out on a single PCS/PVP fiber which was cured at 200−400 °C. Figure 2a−d shows TEM images of thermal-cured fiber as a function of the PCS concentration. All of the cured fibers exhibited uniform core−sheath structures with PCS core encapsulated by an outer PVP shell.

The overall and inner core diameters of cured fiber obtained from 10 wt % PCS droplets entrapped within an aqueous PVP solution were found to be 454 and 214 nm, respectively (Figure 2a). As the concentration of the PCS droplets increased to 20 and 30 wt %, the diameters of PCS/PVP composite fibers also incline to increase (Figure 2b,c). The resultant calcined SiC fibers also exhibited thicker diameters as compared to SiC fibers prepared using 10 wt % PCS droplets. The scanning TEM image and EDS line profiles across the composite fiber containing

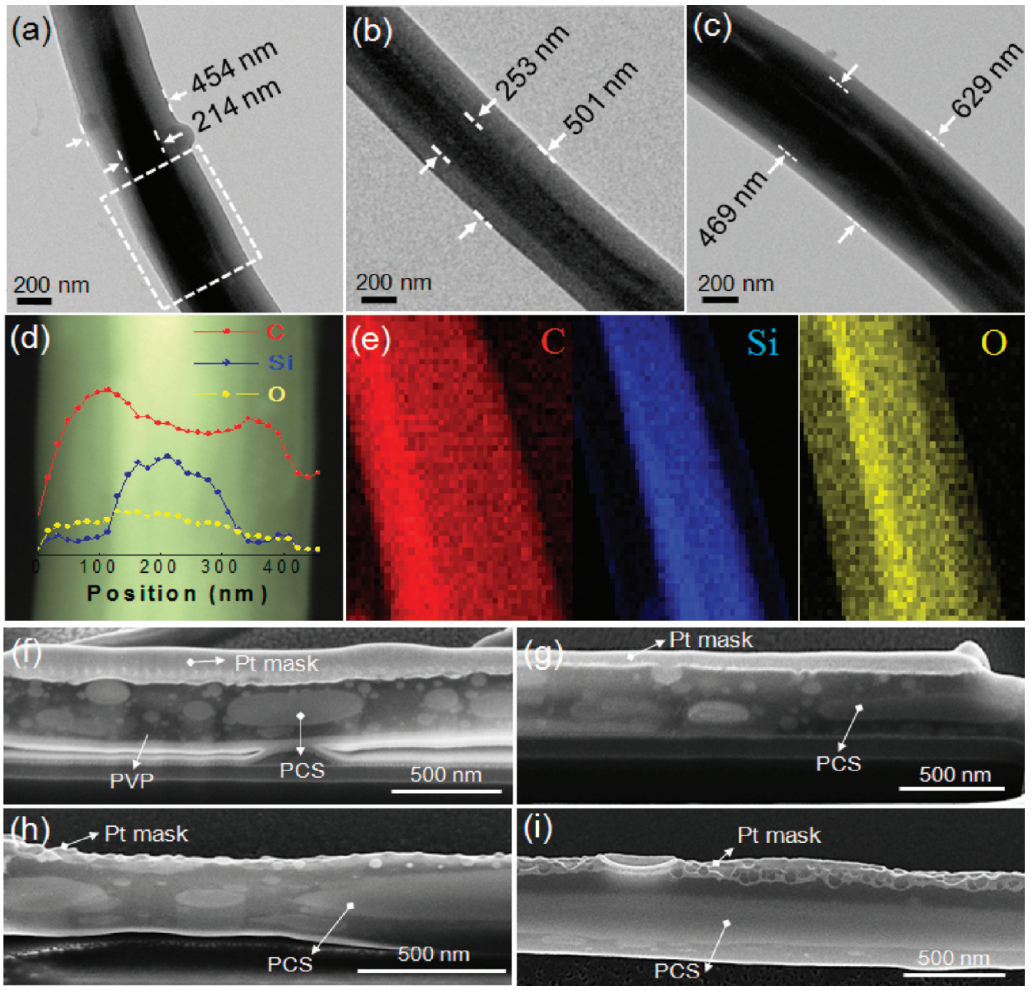

Figure 2. TEM images of a thermal-cured PCS/PVP composite fiber. The concentrations of PCS droplets were (a) 10, (b) 20, and (c) 30 wt % with respect to an aqueous PVP solution, respectively; (d) STEM image and EDS line profiles across a cured composite fiber (dotted area in image a); (e) TEM/EDS mapping of C, Si, and O content of the dotted area in image a. A small amount of sodium (0.15 at %) and sulfur (0.10 at %) originating from the surfactants were detected; FIB cross-section image of (f) as-spun PCS(10 wt %)/PVP composite fiber; (g) thermal-cured PCS(10 wt %)/PVP composite fiber at 200 °C in air for 5 h; (h) calcined PCS(10 wt %)/PVP composite fiber in N_2 at 300 °C for 1 h, and (i) calcined PCS(10 wt %)/PVP composite fiber in N_2 at 400 °C for 1 h.

10 wt % PCS droplets reveal that the cured fiber mainly consists of Si, C and O components (Figure 2d). The outer PVP fiber matrix is mostly made of carbon. In the inner core position, strong Si intensity was observed. This observation is in good agreement with the TEM-EDS mapping of Si (blue dots), C (red dots) and O (yellow dots) (Figure 2e). In a further investigation of the longitudinal cross-section image of PCS(10 wt %)/PVP composite fiber, we carried out focused ion beam (FIB) milling processing (Figure 2f–i). As shown in Figure 2f, inner PCS droplets entrapped in the as-spun PVP fiber showed two distinctive features, i.e., a round shape with small size distribution (20–200 nm) and an elongated elliptical shape (width of 100–200 nm and length of 200–500 nm). As the heat-treatment temperature exceeded to 200 °C, small PCS droplets tended to aggregate gradually, resulting in long stripe-shaped PCS fibrils at 400 °C (Figure 2(h-i), see detail in Figure S2 in the Supporting Information)

This interesting feature can be explained through an investigation of two effects; 1) low internal viscosity able to accelerate the diffusion of PCS segment, and 2) the molecular interactions between the PCS and PVP interface during the thermal decomposition process. In general, polar side groups in polymer chains are known to enhance the intermolecular force and suppress chain fluctuation, leading to a decrease in the flexibility of polymer chains and an increase of their internal viscosity. In the case of PVP, above 200 °C, a certain fraction of the pyrrolidone rings (side chain) in PVP are removed, after which unsaturated carbon backbones in the chains appear.[14] Thus, the diffusion rate of PCS segments are accelerated, resulting in the formation of larger PCS droplets during the thermal degradation of the PVP segments, which reduces their initial interfacial tension against the PVP matrix. For these reasons, polymer migration can be greatly enhanced by the thermal fluctuations of PVP and PCS segments at an elevated temperature (200–400 °C). Further investigations should be carried out to clarify the interdiffusion mechanism between PCS droplets and the PVP matrix. Interestingly, at a concentration of 30 wt % PCS droplets, the diameters of the overall and the elliptical PCS droplets also increased due to the increased emulsion droplet size (see Figure S3 in the Supporting Information).

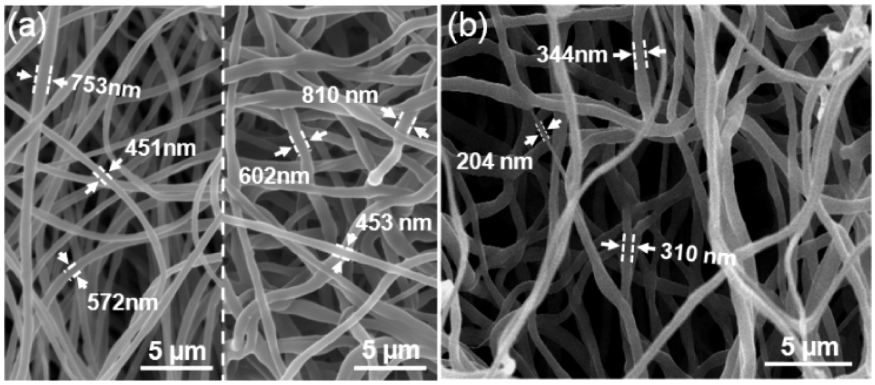

Figure 3. (a) SEM image of the as-spun composite fiber mats (left) and thermal-cured composite fiber mats (right); (b) SEM image of SiC fiber mats calcined at 1600 °C.

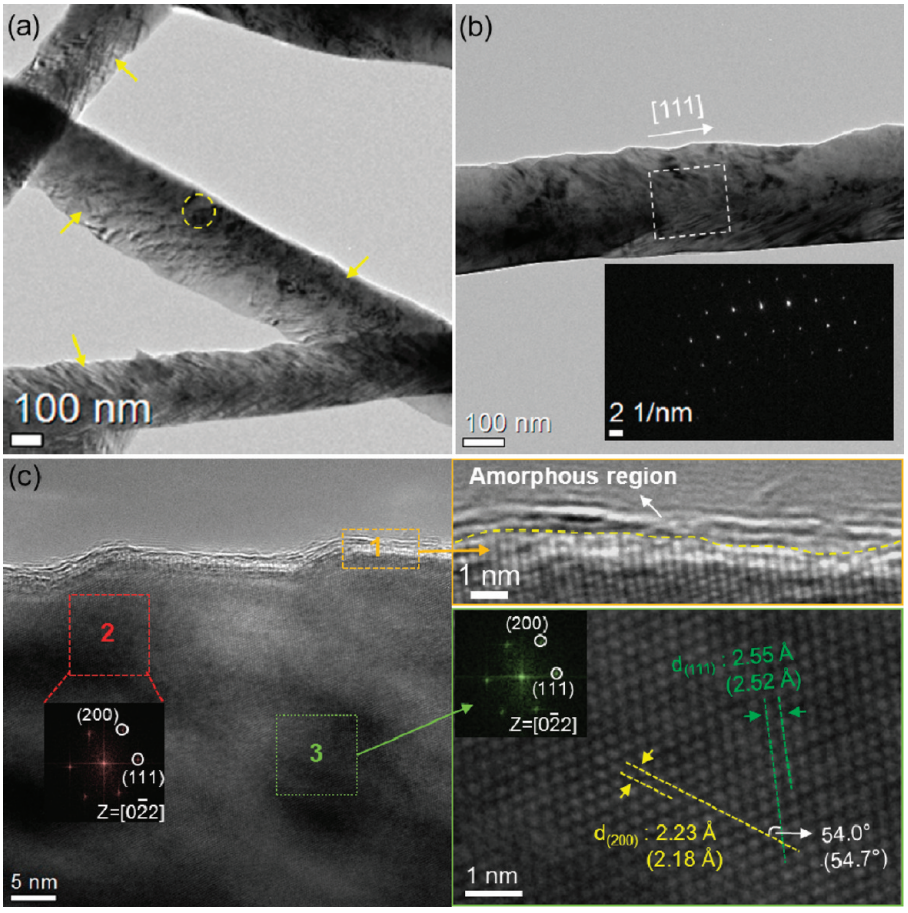

Figure 4. (a, b) TEM images of the SiC fibers. The atomic ratio (%) of Si/C in the dotted circle area is 47:53. Moiré patterns are indicated by the yellow arrows. The [111] crystal orientation of SiC is indicated by the white arrow. The inset is the SAED pattern of the dotted area selected in image b. (c) HR-TEM image of a SiC fiber. Enlarged high-magnification image of area (1); see right upper corner. The FFT diffraction patterns for areas 2 and 3 are shown as insets in the left bottom corner and right middle corner, respectively. The lattice fringe of area 3 is clearly visible (right bottom corner). The values in parentheses correspond to the theoretical results.

Images a and b in Figure 3 show FE-SEM images of the SiC fiber mats during each process step. The as-spun PCS(10 wt %)/PVP composite fibers exhibit randomly oriented fibers in the form of nonwoven mats with diameters ranging from 451 to 753 nm (Figure 3a, left). Surface morphologies of cured fibers were not changed as compared to the pristine fibers (Figure 3a, right). Calcination of the composite fibers at 1600 °C in an Ar atmosphere resulted in SiC fibers due to the crystallization of PCS into SiC and the decomposition of the PVP matrix. Thus, the diameter of SiC nanofiber was slightly reduced by the elimination of the PVP matrix as well as by the densification of the inner SiC. It ranged from 204 to 344 nm while the continuity of the SiC remained in the range of several hundred micrometers. The calcined SiC fiber mats exhibited a high

crystallinity (see Figure S4, XRD pattern, in the Supporting Information).

To investigate the microstructure of the SiC fibers in detail, TEM characterization studies were conducted. Figure 4a shows representative TEM micrographs of SiC fibers. These SiC fibers show Moiré patterns (arrows in Figure 4a), which are clear evidence of the presence of dislocations and stacking faults in the fiber.[15] This is consistent with the XRD result. Indeed, Wang et al. reported that more stacking faults were found in the relatively small diameter of the SiC whisker (~0.2 μm) because increasing the specific lateral surface area of the whiskers while decreasing the diameter can enhance the formation of stacking faults in SiC whiskers.[15b] The selected area electron diffraction (SAED) pattern (inset of Figure 4b) demonstrates that the SiC fiber is a single-crystalline phase (details in Figure S5, Supporting Information). The microstructure of the SiC fiber is clearly observable even at higher magnifications, as shown in Figure 4c. A fast Fourier transform image (FFT) of the near surface area (2, red dotted box) and interior (3, green dotted box) area in the SiC fiber exhibits clear electron diffraction spots, indicating a cubic structure of crystalline SiC, as characterized by the (111) and (200) planes. The outer surface of the SiC fiber exhibits a uniform amorphous phase with a thickness of less than 1 nm, as indicated by the orange (1) box image in Figure 4c. This may indicate the presence of residual carbon. Lattice fringes are clearly visible and are identified with the crystallographic planes of the cubic SiC structure (right bottom corner image in Figure 4c). Lattice planes with interplanar distances of 2.55 and 2.23 Å and an angle of 54° can be observed in the lattice fringe (green dotted box); these correspond respectively to the (111) and (200) planes of the β(3C)-SiC crystal structures.

In summary, this study reported the facile synthesis of a single-crystal β(3C)-SiC submicrofiber via the electrospinning of PCS droplets entrapped within an aqueous PVP solution. Low-molecular weight PCS micelles in emulsion electrospinning played an important role in forming the continuous and dense core structure, resulting in pure SiC fibers. This simplicity of the techniques outlined in this report offers new means of preparing novel single-crystalline β(3C)-SiC fibers with a diameter less than 350 nm. Single-crystalline β(3C)-SiC fibers have considerable potential in diesel particulate filter and ceramic fiber separator requiring high mechanical and thermal stability.

■ ASSOCIATED CONTENT

Supporting Information. Experimental procedures, thermogravimetric analysis (TGA), focused-ion beam (FIB)-SEM images, X-ray diffraction(XRD) pattern, TEM image, and SAED pattern images. This material is available free of charge via the Internet at http://pubs.acs.org.

■ AUTHOR INFORMATION

Corresponding Author

*E-mail: idkim@kaist.ac.kr.Fax: +82-42-350-3310. Tel: +82-42-350-3329.

■ ACKNOWLEDGMENT

This work was supported by a grant from the cooperative R&D Program (B551179-10-01-00) funded by the Korea Research Council Industrial Science and Technology, Republic of Korea. This research was supported by a grant from the Fundamental R&D Program for Core Technology of Materials funded by the Ministry of Knowledge Economy, Republic of Korea.

■ REFERENCES

(1) (a) Mitomo, M.; Kim, Y.-W.; Hirotsuru, H. *J. Mater. Res.* **1996**, *11*, 1601. (b) Pol, V. G.; Pol, S. V.; Gedanken, A. *Chem. Mater.* **2005**, *17*, 1797. (c) Krawiec, P.; Geiger, D.; Kaskel, S. *Chem. Commun.* **2006**, 2469. (d) Sternitzke, M. *J. Eur. Ceram. Soc.* **1997**, *17*, 1061. (e) Krawiec, P.; Weidenthaler, C.; Kaskel, S. *Chem. Mater.* **2004**, *16*, 2869. (f) Shi, Y.; Meng, Y.; Chen, D.; Cheng, S.; Chen, P.; Yang, H.; Wan, Y.; Zhao, D. *Adv. Funct. Mater.* **2006**, *16*, 561. (g) Kamperman, M.; Garicia, C. B. W.; Du, P.; Ow, H.; Wiesner, U. *J. Am. Chem. Soc.* **2004**, *126*, 14708. (h) Yamamoto, T.; Kitaura, H.; Kodera, Y.; Ishii, T.; Ohyanagi, M.; Munir, Z. A. *J. Am. Ceram. Soc.* **2004**, *87*, 1436.

(2) (a) Vanhaecke, E.; Ivanova, S.; Deneuve, A.; Ersen, O; Edouard, D.; Wine, G.; Nguyen, P.; Pham, C.; Pham-Huu, C. *J. Mater. Chem.* **2008**, *18*, 4654. (b) Kawamura, H.; Samukawa-machi U.S. Patent 5 652 250, 1997.

(3) (a) Zhou, W. M.; Fang, F.; Hou, Z. Y.; Yan, L. J.; Zhang, Y. F. *IEEE Trans. Electron Devices* **2006**, *27*, 463. (b) Rogdakis, K.; Bescond, M.; Bano, E.; Zekentes, K. *Nanotechnology* **2007**, *18*, 475715. (c) Elford, A.; Mawby, P. A. *Microelectron. J.* **1999**, *30*, 527.

(4) Li, G.-Y.; Li, X.-D.; Chen, Z.-D.; Wang, J.; Che, R.-C. *J. Phys. Chem. C* **2009**, *113*, 17655.

(5) Yoon, B.-H.; Park, C.-S.; Kim, H.-E. *J. Am. Ceram. Soc.* **2007**, *90*, 3759.

(6) Cui, H.; Sun, Y.; Yang, G. Z.; Chen, J.; Jiang, D.; Wang, C. X. *Chem. Commun.* **2009**, 6243.

(7) (a) He, D.; Hu., B; Yao, Q.-F.; Wang, K.; S-H., Y. U. *ACS Nano* **2009**, *3*, 3993. (b) Ramaseshan, R.; Sundarrajan, S.; Jose, R; Ramakrishna, S. *J. Appl. Phys.* **2007**, *102*, 111101. (c) Shui, J.; Li, J. C. M. *Nano Lett.* **2009**, *9*, 1307.

(8) (a) Kang, P.-H.; Jeun, J.-P.; Seo, D.-K.; Nho, Y.-C. *Radiat. Phys. Chem.* **2009**, *78*, 493. (b) Shin, D.-G.; Riu, D.-H.; Kim, H.-E. *J. Ceram. Proc. Res.* **2008**, *9*, 209. (c) Eick, B. M.; Youngblood, J. P. *J. Mater. Sci.* **2009**, *44*, 160.

(9) (a) Li, J.; Zhang, Y.; Zhong, X.; Yang, K.; Meng, J.; Cao, X. *Nanotechnology* **2007**, *18*, 245606. (b) Lee, S.-H.; Yun, S.-M.; Kim, S. J.; Park, S.-J.; Lee, Y-S *Res. Chem. Intermed.* **2010**, *36*, 731.

(10) (a) Sy, J. C.; Klemm, A. S; Shastri, V. P. *Adv. Mater.* **2009**, *21*, 1814. (b) Kriegel, C.; Kit, K. M.; McClements, D. J.; Weiss, J *Langmuir* **2009**, *25*, 1154. (c) Angeles, M.; Cheng, H.-L.; Venlankar, S. S. *Polym. Adv. Technol.* **2008**, *19*, 728. (d) Xu, X.; Zhuang, X.; Chen, X.; Yang, L.; Xu, X.; Wang, X.; Yang, L.; Jing, X. *Macromol. Rapid Commun.* **2006**, *27*, 1637. (e) Xu, X.; Yang, L.; Xu, X.; Wang, X.; Chen, X.; Liang, Q; Zeng, J.; Jing, X. *J. Controlled Release* **2005**, *108*, 33. (f) Yan, S.; Xiaoqiang, L.; Shuiping, L.; Xiumei, M.; Ramakrishna, S. *Colloids Surf., B* **2009**, *73*, 376.

(11) (a) Kockrick, E.; Krawiec, P.; Petasch, U.; Martin, H.-P.; Herrmann, M.; Kaskel, S. *Chem. Mater.* **2008**, *20*, 77. (b) Kockrick, E.; Frind, R.; Rose, M; Petasch, U.; Bohlmann, W.; Geiger, D.; Herrmann, M.; Kaskel, S. *J. Mater. Chem.* **2009**, *19*, 1543.

(12) Bakumov, V.; Schwarz, M.; Kroke, E. *J. Eur. Ceram. Soc.* **2009**, *29*, 2857.

(13) (a) de Andrade, M. L.; Atvars, T. D. Z. *Macromolecules* **2004**, *37*, 9626. (b) Wang, S.-Q.; Shi, Q. *Macromolecules* **1993**, *26*, 1091. (c) Bognitzke, M.; Frese, T.; Steinhart, M.; Greiner, A.; Wendorff, J. H. *Polym. Eng. Sci.* **2001**, *41*, 982.

(14) Peniche, C.; Zaldivar, D.; Pazos, M.; Paz, S.; Bulay, A.; Roman, J. S. *J. Appl. Polym. Sci.* **1993**, *50*, 485.

(15) (a) Choi, H.-J.; Lee, J.-G. *Ceram. Int.* **2000**, *26*, 7. (b) Wang, L.; Wada, H.; Allard, L. F. *J. Mater. Res.* **1992**, *7*, 149.